Science of the Total Environment 768 (2021) 145312

Contents lists available at ScienceDirect

Science of the Total Environment

journal homepage: www.elsevier.com/locate/scitotenv

Impact of extreme floods on plants considering various influencing factors downstream of Luhun Reservoir, China

Yadong Zhang [a], Zongkun Li [a,b,*], Wei Ge [a], Xudong Chen [a], Hongyin Xu [a], Xinyan Guo [a], Te Wang [a]

[a] *School of Water Conservancy Engineering, Zhengzhou University, Zhengzhou 450001, China*
[b] *School of Software, Zhengzhou University, Zhengzhou 450002, China*

HIGHLIGHTS

- The factors affecting the impacts of extreme floods on plants were simplified into six main influencing factors
- A method was proposed to evaluate the impacts of extreme floods on plants
- The impacts of extreme floods on plants change with space and time due to changes in various influencing factors

GRAPHICAL ABSTRACT

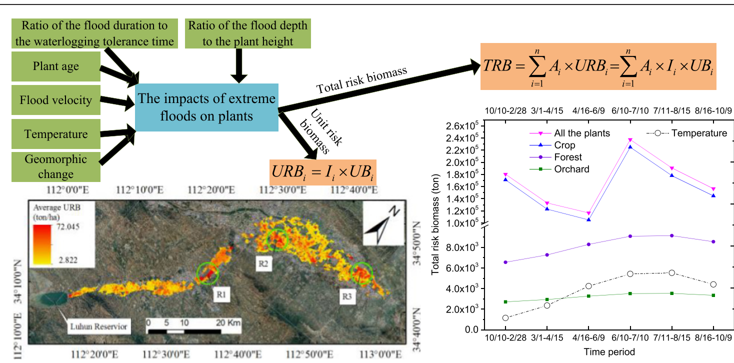

ARTICLE INFO

Article history:
Received 16 November 2020
Received in revised form 16 January 2021
Accepted 16 January 2021
Available online 21 January 2021

Editor: Fernando A.L. Pacheco

Keywords:
Environmental flood risk
Flood consequence
Impact evaluation method
Plant

ABSTRACT

Extreme floods caused by dike or dam breaks have led to substantial damage to various types of vegetation, including forests, orchards, grass, and crops. Many factors affect the impacts of extreme floods on plants, e.g., flood parameters, plant characteristics and natural factors. However, these factors have never been systematically analyzed or considered when evaluating the impacts of extreme floods on plants. Firstly, we summarized the main influencing factors and simplified them into six categories: temperature, geomorphic change, plant age, flood velocity, ratio of the flood depth to the plant height, and ratio of the flood duration to the plant waterlogging tolerance time. Secondly, we proposed the two indices of unit risk biomass (*URB*) and total risk biomass (*TRB*) to represent the impacts of floods on plants regionally and over the entire inundated area, respectively. In addition, the calculation methods of *URB* and *TRB* considering plant biomass and the comprehensive influence coefficient (*I*) were put forward. To calculate *I*, we considered the six influencing factors with different weights according to their importance and varying conditions. The flood parameters and geomorphic changes caused by a simulated dam-break flood of Luhun Reservoir in China were then calculated. Furthermore, we divided a year into six time periods according to the species and growth characteristics of the plants in the inundated area. Then we evaluated the impacts of the dam-break flood on the plants during each period. The results showed that: (a) the *URB* varied with space in the inundated area; (b) because of the large inundation area of crops, the *TRB* was far greater than that of forests and orchards and affected the *TRB* of the whole inundated area; and (c) both the *URB* and *TRB* changed with time with the changes in crop species, crop parameters and temperature.

1. Introduction

Climate change is predicted to cause an increase in the intensity of precipitation events (Tebaldi et al., 2006; Vervuren et al., 2003), which

* Corresponding author at: School of Water Conservancy Engineering, Zhengzhou University, No. 100 Science Avenue, Zhengzhou 450001, China.
E-mail address: lizongkun@zzu.edu.cn (Z. Li).

https://doi.org/10.1016/j.scitotenv.2021.145312
0048-9697/

will lead to more flooding events globally (Ye et al., 2011; Pucciariello et al., 2014). Among them, extreme floods caused by dam or dike breaches will cause extensive damage to human life, economic activity, and the environment (Ge et al., 2020a, 2020b, 2021). An important aspect of environmental flood risk is the impact on plants (Scheuer et al., 2011). The extreme flood of the Rhine River was recorded to cause the death of a large number of trees in 1999 (Kramer et al., 2008). Four floods were observed to wash down the willows in the floodplain of the Kako River Basin in Japan from 2009 to 2011 (Miyamoto and Kimura, 2016). Therefore, floods are a significant environmental threat for plants (Pucciariello et al., 2014) and the most frequent type of natural disaster in many areas (Lugeri et al., 2010). Moreover, 27% of cropland is affected by floods worldwide (Pasley et al., 2020). Floods not only cause plant death but also limit the accumulation of plant biomass (Xu et al., 2015; Pires et al., 2018), thus reducing their biomass and yield (Watson et al., 1976; Posthumus et al., 2010; Pucciariello et al., 2014).

Many factors affect the impacts of floods on plants (Setter and Waters, 2003). Singh and Ghildyal (1980) found that the waterlogging tolerance of plants, temperature, plant age, and flood duration were the main influencing factors. Kramer et al. (2008) ranked the importance of flood duration, depth, and velocity and determined that flood duration and velocity were the most and least important influencing factors, respectively. Karrenberg et al. (2010) analyzed the impact of erosion caused by floods on willows and poplars. Moreover, sediment burial, plant height, and other factors also have a significant influence on the impacts of floods on plants (Gattringer et al., 2017; K. Li et al., 2018; Zacks et al., 2018). However, these previous studies only analyzed a portion of the influencing factors (Winkel et al., 2017; Higgisson et al., 2018).

The impact of floods on plants is a significant aspect of environmental flood risk. The evaluation methods used are risk index analysis (Kubal et al., 2009; Scheuer et al., 2011) and weight scoring (Z. Li et al., 2018; Wu et al., 2019). The risk index analysis method was used in the city of Leipzig in Saxony, Germany (Scheuer et al., 2011). The inundated areas of floods divided into 10×10 m grids and considering whether the forest was submerged or not, a Boolean yes/no damage function was applied to each grid. Therefore, the damage value for each grid was between 0 and 1, and different damage values were calculated for floods with different return periods. Then, the damage value was multiplied by the corresponding flood probability, and the values were summed to produce the risk index (0 to 1) representing the impact of floods on forests (Meyer et al., 2009).

The weight scoring method was applied to Shaheji Reservoir, China (Wu et al., 2019). It used the vegetation coverage rate of the inundated area multiplied by the weigh (0 to 1) determined according to the experience of experts to represent the impacts of extreme floods on plants (Li et al., 2020). However, different forests usually contain varied biomass or timber volume (Visser and Peterson, 2015; Pires et al., 2018). Therefore, floods may have diverse impacts on different forests even with the same inundated area (Hook, 1984; Copolovici and Niinemets, 2010). Overall, neither the risk index nor the vegetation coverage rate can accurately represent the impact degree of extreme floods on plants. Moreover, the risk index analysis only considered the impacts of floods on forests (Scheuer et al., 2011), and other vegetation, such as grass, shrubs, fruit trees, and crops, were ignored. Ignoring other plants can lead to a serious underestimation of the impacts of floods on plants in the entire inundated area, especially in areas with few forests.

Therefore, the current methods for evaluating the impacts of extreme floods on plants are inaccurate, and the indices used to represent the impact degree are unreasonable. In addition, all the influencing factors were ignored in the current evaluation methods (Scheuer et al., 2011), which will lead to considerably errors in the evaluation results. Furthermore, some factors change significantly during the year, e.g., species, age, and average height of plants, and temperature (Setter and Waters, 2003; Zaidi et al., 2004; Wang et al., 2017), which leads to varied impacts with time even with the same flood parameters. However, these changes in the influencing factors have not been considered in the current evaluation methods (Li et al., 2020).

Extreme floods cause substantial impacts on all vegetation in the inundated area (Dixon, 2003). The impact degree varies with the plant species and is affected by many factors (Gattringer et al., 2017; Zacks et al., 2018). However, none of these is considered in the current methods for evaluating the impacts of extreme floods on plants, resulting in indices that cannot reflect the impact degree reasonably and the evaluation results that are not accurate enough. Therefore, the primary objectives of this study are to (1) analyze the main factors affecting the impacts of flooding on plants; (2) propose a new evaluation method that uses new indices to represent the impact of extreme floods on the vegetation.

2. Materials and methods

2.1. Study site

Luhun Reservoir (34°08′N, 112°03′E) is a Large (1) type class reservoir with a capacity of 1.316 billion m^3 at flood check level, in Luoyang City, China (Fig. 1). The study area is approximately 400 km^2 and is hilly between the dam site and Luoyang City with a plain between Luoyang City and the Yellow River. The elevation of the Yihe river decreases from 280 m to 80 m from the dam site to the Yellow River with an average slope of 0.0017. The study area is in the temperate zone of the northern hemisphere, with mean annual precipitation, evaporation, and temperature of 650.2 mm, 763.4 mm, and 15.0 °C, respectively (National Meteorological Center, 2020). The precipitation is concentrated from June to September. Farmland, town, and forest (including arbor forests and orchards) are the primary land-use types. Poplar is the predominant tree species (Henan Provincial People's Government, 2018); wheat and rape are the primary winter crops; maize, peanuts, and beans are the main summer crops; apple, pear, peach, and grape trees are the predominant fruit trees (Statistics Bureau of Henan Province and Henan survey team of National Bureau of Statistics, 2019).

2.2. Numerical simulation of flood parameters

HEC-RAS was used to simulate the dam-break flood process of Luhun Reservoir (US Army Corps of Engineers, Hydrologic Engineering Center, 2016). The data used for simulation included the DEM of the reservoir (Fig. 2), which can be downloaded from the Geospatial Data Cloud website (http://www.gscloud.cn/sources/?cdataid=302&pdataid=10), and the dam breach parameters. We assumed that the dam would break due to overtopping, and the breach top width, bottom width, depth and failure time were respectively calculated as 330.3 m, 230.9 m, 48.9 m and 9.2 h according to the method proposed by Xu et al. (2009). The calculated dam-break flood process is shown in Fig. 3.

MIKE 21 consists of two components. In which MIKE ZERO was used to transfer the dam-break flood process to the inflow file, transfer the land-cover map to the sand layer thickness file, Manning coefficient file, and infiltration rate file (DHI Water and Environment, 2007a), and transfer the DEM of the study area to the mesh file, which includes many meshes. All the files generated by MIKE ZERO are used in MIKE 21FM to simulate the flood route and geomorphic changes (DHI Water and Environment, 2007b; DHI Water and Environment, 2007c). The land-cover map can be downloaded from the Resource and environment data cloud platform website (http://www.resdc.cn/data.aspx?DATAID=264), as shown in Fig. 4.

The infiltration rate file included the steady infiltration rate of different land use types. The steady infiltration rate of cropland (288.0 mm/d) and river (2566.0 mm/d) were the results of soil infiltration rate tests conducted by Su et al. (2004) and Luoyang Water Resources Surveying and Designing Co., Ltd. (2020) in the study area, respectively.

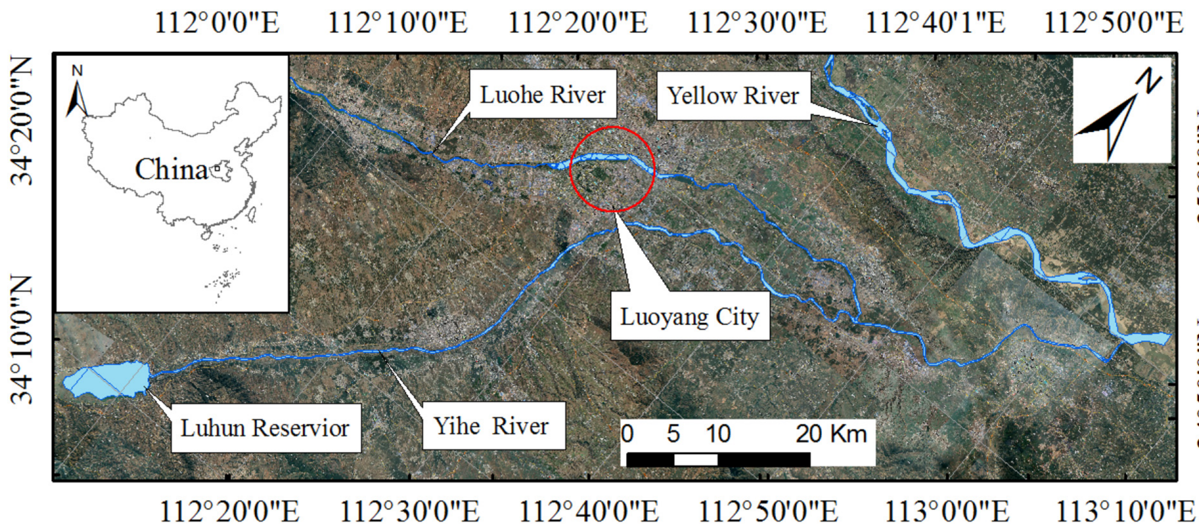

Fig. 1. Location of Luoyang City and Luhun Reservoir, China.

The rate for the forest of 567.3 mm/d was calculated according to the ratio of forest to cropland deduced by Sun et al. (2018).

The soil in the study area is collapsible loess with particles of predominantly coarse silt and sand (account for 74% of the total soil particles), thickness of 6 m, and average porosity of 0.49 (Luo, 2008; Feng et al., 2009; Ministry of Housing and Urban-rural Development of the People's Republic of China, General Administration of Quality Supervision, Inspection and Quarantine of the People's Republic of China, 2016). Therefore, we regarded all the soil in the study area as sand. According to the grading curve conducted by Luoyang Water Resources Surveying and Designing Co., Ltd. (2020) in the study area, the median grain diameter D_{50} of the study area soil was 0.028 mm.

ArcGIS was used to extract the calculated results of MIKE 21, specifically, the flood parameters (depth, velocity, and duration) and magnitude of the geomorphic changes (erosion depth or deposition depth) of each mesh in the inundated area. In addition, the inundated area map was intersected with a land-cover map to obtain the land use type of each mesh with ArcGIS. Furthermore, it was used for mapping to show the flood parameters and evaluation results of each mesh.

2.3. Analyzing the main factors affecting the impacts of floods on plants

We determined the factors influencing the impacts of flood on plant growth from the previous literature. These factors may positively or negatively affect the impacts of floods on the vegetation, that is, their values may be proportional or inversely proportional to the impact degree. Therefore, the relationship between these factors and the impact degree are expressed as “proportional” or “inversely proportional” in Table 1.

Erosion and deposition are both geomorphic changes, so “geomorphic change” was used to represent them. Flood depth and plant height are two opposite influencing factors, as well as the flood duration and waterlogging tolerance time of plants. Therefore, we respectively used the ratio of flood depth to plant height and the ratio of flood duration to waterlogging tolerance time of plants to represent these categories. Finally, we simplified all the main influencing factors into six categories, namely temperature (T), geomorphic change (G), plant age (A), flood velocity (V), ratio of the flood depth to the plant height (D), and ratio of the flood duration to the waterlogging tolerance time (F).

When most of the roots are exposed by erosion, the whole plant is buried by sediment, or the flood duration exceeds the waterlogging

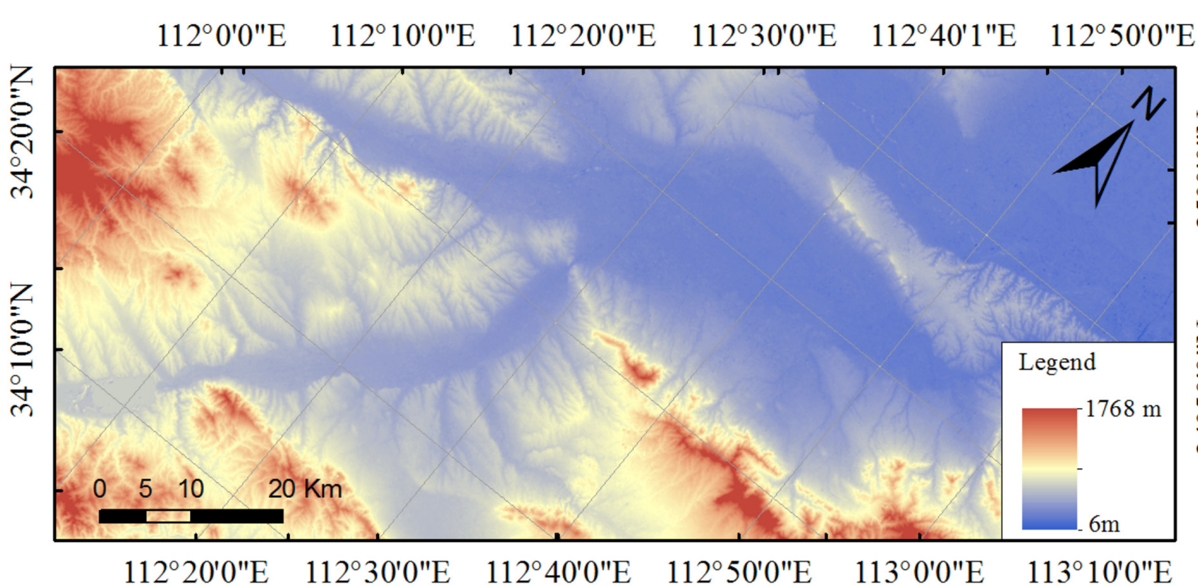

Fig. 2. 30 m-precision DEM of the study area (Geospatial Data Cloud, 2020).

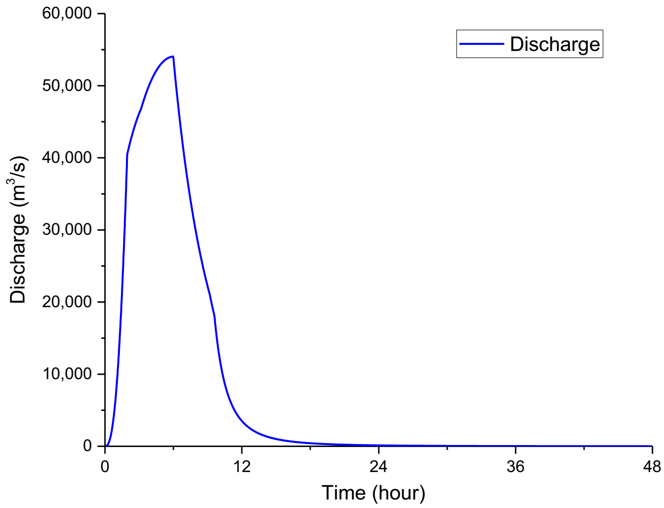

Fig. 3. Dam-break flood process.

tolerance time of the plant, the plant may die. Therefore, *G* and *F* were regarded as the two most important factors.

Waterlogging decreases oxygen diffusion into the soil and leads to hypoxia of the plant roots (Najeeb et al., 2015). High temperatures further aggravate this phenomenon (Rapacz et al., 2014; Gattringer et al., 2017). However, for every 10 °C increase in temperature, the respiration rate and oxygen consumption of the plants will double to triple (Setter and Waters, 2003; Wang et al., 2017; Ben-Noah and Friedman, 2018). In addition, high temperatures increase the transpiration of plants, while the plant roots cannot meet the high evaporative demand due to the stomatal closure induced by waterlogging (Singh and Ghildyal, 1980; Wang et al., 2017). Therefore, high temperatures can easily cause plant death. Plant age directly affects the waterlogging tolerance of plants. With the increase in plant age, the roots become more developed, and the reserve organs that can sequestrate carbon became larger (Mauchamp et al., 2001). Therefore, *T* and *A* were regarded as two moderately important factors.

Kramer et al. (2008) found that flood duration, depth, and velocity accounted for 19%, 11%, and 8%, respectively, of tree injury and mortality. The effect of flood depth was similar to that of flood velocity but far less than that of flood duration. Therefore, *V* and *D* were regard as two less important factors.

2.4. Evaluation of the impacts of floods on plants

All six influencing factors were considered in a comprehensive influence coefficient I ($0 \le I \le 1$). $I = 0$ and 1 respectively mean that the flood causes no plant loss and complete plant biomass loss (die) in a region.

2.4.1. Calculation of I

We used different maximum impact values to represent the importance of the influencing factors. Obviously, more important factors have a greater influence on the impacts of extreme floods on vegetation. According to Section 2.3, *G* and *F*, *T* and *A*, *V* and *D* were regarded as the two most important, moderately important, and least important factors, respectively. Kramer et al. (2008) found that flood duration and velocity accounted for 19% and 8%, respectively, of tree injury and mortality. While flood duration and velocity were the most important and least important factors. Therefore, we give the most important, medium important and less important factors the maximum weights of 10, 6, and 3, respectively. Therefore, the maximum impact value of *G* and *F*, *T* and *A*, *V* and *D* were 10, 6, and 3, respectively.

The impacts of extreme floods on plants depend on six factors, each of which has a different actual impact. In addition, the actual impact of a factor varies in different situations, e.g., *T* at 10 and 20 °C. Therefore, W_G, W_F, W_V, W_D, W_T, and W_A were used to represent the actual impact value of *G*, *F*, *V*, *D*, *T*, and *A*, respectively, which were all between zero and the corresponding maximum impact value.

Of all the factors, only *G* and *F* could directly cause plant death. In this situation, the actual impact values of *G* and *F* all reach the maximum value, leading to *I* reaching the maximum value, namely when W_G or $W_F = 10$, $I = 1$. Therefore, the total actual impact value of the six factors ($W_T + W_G + W_A + W_V + W_D + W_F$) is between 0 and 38 ($38 = 10 + 10 + 6 + 6 + 3 + 3$). When the total actual impact value reaches 75% of the maximum value, it will cause extensive damage to the vegetation and is likely to cause plant death, namely when $W_T + W_G + W_A + W_V + W_D + W_F = 28.5$, $I = 1$. Therefore, we proposed to calculate *I* using Eq. (1).

$$\begin{cases} Max\{\mathrm{W_G}, \mathrm{W_F}\} = 10, \quad \mathrm{I} = 1 \\ Max\{\mathrm{W_G}, \mathrm{W_F}\} < 10, \begin{cases} \mathrm{W_T} + \mathrm{W_G} + \mathrm{W_A} + \mathrm{W_V} + \mathrm{W_D} + \mathrm{W_F} \ge 28.5, \mathrm{I} = 1 \\ \mathrm{W_T} + \mathrm{W_G} + \mathrm{W_A} + \mathrm{W_V} + \mathrm{W_D} + \mathrm{W_F} < 28.5, \mathrm{I} = \\ \quad (\mathrm{W_T} + \mathrm{W_G} + \mathrm{W_A} + \mathrm{W_V} + \mathrm{W_D} + \mathrm{W_F})/28.5 \end{cases} \end{cases} \tag{1}$$

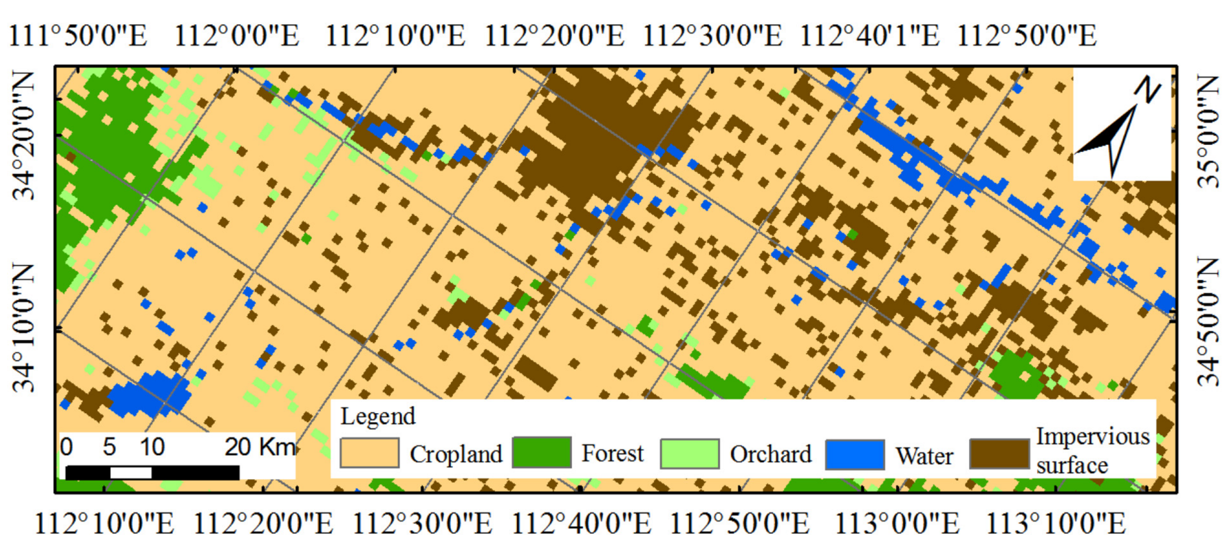

Fig. 4. 1 km-precision land-cover map of the study area (Resource and environment data cloud platform, 2020).

Table 1
Factors affecting the impact of floods on plants.

Factors	Influence analysis	References
Temperature	Proportional	James and David, 1970; Falloon and Grogan, 1991; Musgrave and Ding, 1998; Setter and Waters, 2003; Auchincloss et al., 2012; Gattringer et al., 2017; Wang et al., 2017; Winkel et al., 2017
Erosion	Proportional	Dixon, 2003; Ahn et al., 2007; Miyamoto and Kimura, 2016; K. Li et al., 2018
Deposition	Proportional	Dixon, 2003; Ahn et al., 2007; Vreugdenhil et al., 2006; K. Li et al., 2018
Plant age	Inversely proportional	Singh and Ghildyal, 1980; Hook, 1984; Falloon and Grogan, 1991; Mauchamp et al., 2001; Setter and Waters, 2003; Zaidi et al., 2004; Fraser and Karnezis, 2005; Stokes, 2008; Gattringer et al., 2017
Flood velocity	Proportional	Kramer et al., 2008; Miyamoto and Kimura, 2016
Flood depth	Proportional	Casanova and Brock, 2000; Mauchamp et al., 2001; Vreugdenhil et al., 2006; Kramer et al., 2008; Kenow and Lyon, 2010; Auchincloss et al., 2012; Higgisson et al., 2018; Zacks et al., 2018
Plant height	Inversely proportional	Hook, 1984; Higgisson et al., 2018; K. Li et al., 2018
Flood duration	Proportional	Singh and Ghildyal, 1980; Falloon and Grogan, 1991; Casanova and Brock, 2000; Vreugdenhil et al., 2006; Kramer et al., 2008; Auchincloss et al., 2012; Mcdaniel et al., 2016; Higgisson et al., 2018; Zacks et al., 2018
Waterlogging tolerance of plants	Inversely proportional	Singh and Ghildyal, 1980; Hook, 1984; Verhoeven and Setter, 2010; Kenow and Lyon, 2010; Gattringer et al., 2017; Zacks et al., 2018

The actual impact values of these factors are calculated as follows:

(1) W_T

The annual average temperature in most parts of the world is between 0 and 40 °C, except for areas near the Antarctic and Arctic regions (Liu et al., 1980). Flooding at high temperatures causes more plant death and biomass loss than at low temperatures (Beard and Martin, 1970; Auchincloss et al., 2012). Therefore, we used Eq. (2) to calculate W_T.

$$\begin{cases} T \geq 40^{\circ}C, & W_T = 6 \\ 0 < T < 40^{\circ}C, & W_T = T/40 \times 6 \\ T \leq 0^{\circ}C, & W_T = 0 \end{cases} \tag{2}$$

(2) W_G

Plants may die when the deposition depth is greater than plant height or the erosion depth is greater than the distribution depth of 70% of the plant roots (most plant roots are washed out of the soil) (Li et al., 2021). In addition, with an increase in deposition or erosion depth, the vegetation will suffer more damage. Therefore, we used Eq. (3) to calculate W_G.

$$\begin{cases} \begin{cases} G_D \geq P_h, & W_G = 10 \\ G_D < P_h, & W_G = 10 \times G_D/P_h \end{cases} \\ \begin{cases} G_E \geq D_{70}, & W_G = 10 \\ G_E < D_{70}, & W_G = 10 \times G_E/D_{70} \end{cases} \end{cases} \tag{3}$$

where G_D and G_E are the deposition depth and erosion depth, respectively; P_h is the plant height; and D_{70} is the distribution depth of 70% of plant roots.

The calculation of D_{70} for different plants used the function of cumulative vertical distribution of plant roots in soil (Eq. (4)) proposed by Gale and Grigal (1987):

$$Y = 1 - \beta^d \tag{4}$$

where Y is the cumulative distribution proportion of plant roots at depth of d and β is the distribution coefficient (the average β for crops, trees, shrubs, and grass were proposed as 0.961, 0.97, 0.978, and 0.952, respectively, by Jackson et al. (1996)).

(3) W_A

Trees are usually divided into three groups according to plant age, namely young, middle–aged, and mature (Keränen et al., 2015; Munévar et al., 2018), represented by $A = 1$, 2, and 3, respectively. The growth stages of crops are typically divided into four stages of seeding and early growth, late growth or tillering, flowering or tasseling, and yield formation or grain filling (Setter and Waters, 2003; Zaidi et al., 2004). The height of crops increases only slightly from the third to the fourth growth stage, so we merged them into the flowering and yield formation stage. Therefore, crops also could be divided into three groups according to the three growth stages, represented by $A = 1$, 2, and 3, respectively.

Mature trees are more resistant to waterlogging than young ones (Stokes, 2008; Gattringer et al., 2017), and there is a similar trend in crops. The damage caused by the same flood during the early growth stages of crops is greater than that during the late growth stages (Mauchamp et al., 2001; Zaidi et al., 2004). Therefore, with the increases in plant age, plants will suffer less damage. Accordingly, we used Eq. (5) to calculate W_A.

$$W_A = 8 - 2 \times A, \quad 1 \leq A \leq 3 \tag{5}$$

(4) W_V

Nicklisch (2004) classified the flood velocity from 974 cases into three levels, namely moderate (<1.5 m/s), high (1.5 to 4.5 m/s), and very high (>4.5 m/s). A high flood velocity is more likely to cause erosion or wash down plants (Miyamoto and Kimura, 2016; Li et al., 2021). Therefore, with the increase in flood velocity, plants will suffer more damage. On this basis, we used Eq. (6) to calculate W_V.

$$\begin{cases} V \geq 4.5\ m/s, W_V = 3 \\ V < 4.5\ m/s, W_V = V/4.5 \times 3 \end{cases} \tag{6}$$

(5) W_D

With an increase in the ratio of flood depth to plant height, more plants are submerged, and leaves and roots are less exposed to light and oxygen. As a result, respiration and photosynthesis are seriously reduced, which is more likely to cause plant death (Mauchamp et al., 2001). $D \geq 1$ is the most unfavorable case. Therefore, we used Eq. (7) to calculate W_D.

$$\begin{cases} D \geq 1, W_D = 3 \\ D < 1, W_D = D \times 3 \end{cases} \tag{7}$$

(6) W_F

The water tolerance of plants was divided into five classes by Whitlow and Harris (1979). The class of 1, very intolerant; 2, intolerant; 3, moderately tolerant; 4, tolerant; and 5, very tolerant, respectively, indicate that plants can tolerate waterlogging for no more than a few days, one to two weeks, 30 consecutive days, one growing season, or more than one year. Therefore, we regarded the waterlogging tolerance time of classes 1 to 5 as 7, 14, 30, 90, 365 days, respectively. On this basis, the waterlogging tolerance class and time of plants could be converted into each other. In addition, the waterlogging tolerance classes of 806 tree species in the temperate zone of the Northern hemisphere was calculated by Niinemets and Valladares (2006). With an increases in the ratio of flood duration to waterlogging tolerance time of plants, plants will suffer more damage. $F \geq 1$ is the most unfavorable case. Therefore, we used Eq. (8) to calculate W_F.

$$\begin{cases} F \geq 1, \quad W_F = 10 \\ 0 \leq F < 1, W_F = F \times 10 \end{cases} \tag{8}$$

2.4.2. Index used to represent the impacts of floods on plants

Biomass refers to the organic matter (dry weight) of plants in a unit area at a certain time. It is widely used to represent the growth state of the plants (Wang et al., 2018; Golubkina et al., 2020) and effects of various factors on the vegetation (Shi et al., 2004; Han et al., 2017). The biomass of different plant species varies greatly, as well as the same plant species with different ages or growth conditions. Therefore, the impact of floods on plant biomass is more suitable to represent the impact degree than the area, vegetation coverage rate, and risk index.

Combined with plant biomass and *I*, we proposed two indices to quantitatively describe the impacts of floods on plants, namely unit risk biomass (*URB*) and total risk biomass (*TRB*), representing the impacts regionally and over the entire inundated area, respectively. The entire inundated area can be divided into many meshes with MIKE 21. The area and land use type of each mesh can be obtained with ArcGIS. Therefore, we proposed to use Eqs. (9) and (10) to calculate the *URB* of each mesh and the *TRB* of the entire inundated area, respectively.

$$URB_i = I_i \times UB_i \tag{9}$$

where URB_i, and UB_i are the unit risk biomass and the unit biomass of mesh *i*, respectively; and I_i is the comprehensive influence coefficient of the extreme flood on mesh *i*.

$$TRB = \sum_{i=1}^{n} A_i \times URB_i = \sum_{i=1}^{n} A_i \times I_i \times UB_i \tag{10}$$

where *n* is the total number of meshes; and A_i *is* the area of mesh *i*.

The calculation of *URB* and *TRB* comprise three steps:

Step 1 determines the inundated area of extreme floods and divides the entire inundated area into many meshes. MIKE 21 could be used to simulate the evolution process of the extreme flood. The required data and calculation process are described in Section 2.2.

Step 2 analyzes the flood parameters, land use type, and plant parameters of each mesh. Specifically, the flood parameters and land use type of each mesh could be extracted from the calculation results of MIKE 21 with ArcGIS. The details are given in Section 2.2. The collection of the plant parameters (plant species, height, age, waterlogging tolerance time, and unit biomass) of each land use type is discussed in Section 2.5.

Step 3 calculates the *URB* of each mesh and the *TRB* of the entire inundated area. According to the flood parameters and plant parameters of each mesh, the corresponding *I* and *URB* could be calculated with Eqs. (1) and (9), respectively. Then the *TRB* of the inundated area could be calculated using Eq. (10) with the *URB* and area of each mesh.

2.5. Data collection

2.5.1. Unit biomass (UB) of different plants

(1) Crops

The *UB* of crops was calculated as follows (Bi, 2010).

$$UB_C = Y \times RGS \times (1 - W) \tag{11}$$

where UB_C is the unit biomass of crops; *Y* is the yield; *RCS* is the ratio of grain to straw; and *W* is the water content of grain.

The primary winter crops are wheat and rape, and summer crops are maize, peanuts, and beans (Statistics Bureau of Henan Province and Henan survey team of National Bureau of Statistics, 2019). Therefore, we used the unit biomass of the main crops to represent that of all crops. According to Eq. (11), the UB_C of the winter crops and summer crops were calculated as 10.01 and 11.15 ton/ha, respectively (Bi, 2010; Statistics Bureau of Henan Province and Henan survey team of National Bureau of Statistics, 2019).

(2) Forests

The *UB* of forests was calculated as follows (National Development and Reform Commission, 2011; Zhang, 2018).

$$UB_F = VT \times SVD \times BEF \tag{12}$$

where UB_F is the unit biomass of forests; *VT* is the unit timber volume of trees; *SVD* is the timber density; and *BEF* is the biomass ratio of the whole tree to the trunk.

The predominant tree species in the study area is poplar (Henan Provincial People's Government, 2018). Therefore, we used the unit biomass of poplar to represent that of all trees. *VT* equals the total timber volume of trees divided by the total area. The data was from the State Forestry Administration of the People's Republic of China (2013). The values of *SVD* and *BEF* were from the National Development and Reform Commission (2011). According to Eq. (12), the UB_F was calculated as 72.05 ton/ha.

The *UB* of orchards adopted the data of the National Development and Reform Commission (2011), namely 35.21 ton/ha.

(3) Grass and shrubs

The calculation of *UB* of grass and shrubs is similar to that of crops and orchards, respectively.

2.5.2. Plant age

We used winter wheat and maize to represent winter and summer crops because they accounted for 73.5% and 54.4% of the total area, respectively (Statistics Bureau of Henan Province and Henan survey team of National Bureau of Statistics, 2019). Therefore, according to the growth characteristics of winter wheat and maize and Section 2.4.1, the entire life cycle of winter and summer crops were respectively divided into three growth stages with the corresponding time periods (Hu et al., 2008; Shi and Xie, 2009) and plant ages (Table 2).

The average age of the forests in the study area was the weighted average based on the area and age of all the trees of Henan Provence (Henan Provincial Department of Forestry, 2015). There is no age for fruit trees in the statistics, so we considered the average ages of forests and orchards to be the same.

2.5.3. Plant height

According to the plant height parameters (Breuer et al., 2003; Zheng and Xing, 2015) and the area and growth characteristics of the main crops (Hu et al., 2008; Shi and Xie, 2009; Statistics Bureau of Henan Province and Henan survey team of National Bureau of Statistics, 2019), we calculated the average height of the winter and summer crops during three time periods, respectively (Table 2).

The average height of forests adopted the value of the predominant species poplar (Li and Fa, 2011). The heights of fruit trees do not change much after fruiting because of frequent pruning. Tang et al. (2015) proposed the proper height for orchards as approximately 3 m, because the management of taller fruit trees requires more labor (Choi et al., 2014). Therefore, we used 3 m as the average height of the orchards.

Table 2
Plant parameters and temperature within a year.

	Main species	Time period	Growth stage	Plant age	Average height (m)	Average temperature (°C)	Waterlogging tolerance class	Waterlogging tolerance time (day)
Winter crops	Wheat, rape	10/10–2/28	Early growth	1	0.23	5.67	2	14
		3/01–4/15	Late growth	2	0.69	11.58		
		4/16–6/09	Flowering and yield formation	3	1.15	20.84		
Summer crops	Maize, peanuts, and beans	6/10–7/10	Early growth	1	0.33	26.65	1	7
		7/11–8/15	Late growth	2	1.00	27.14		
		8/16–10/09	Flowering and yield formation	3	1.67	21.63		
Orchards	Apple, peach, pear, and grape trees	10/10–2/28	/	1.68	3.00	5.67	1.37	9.57
		3/01–4/15				11.58		
		4/16–6/09				20.84		
		6/10–7/10				26.65		
		7/11–8/15				27.14		
		8/16–10/09				21.63		
Forests	Poplar	10/10–2/28	/	1.68	11.15	5.67	2.49	21.79
		3/01–4/15				11.58		
		4/16–6/09				20.84		
		6/10–7/10				26.65		
		7/11–8/15				27.14		
		8/16–10/09				21.63		

2.5.4. Waterlogging tolerance of plants

The waterlogging tolerance time of the winter and summer crops were determined according to that of wheat and maize, which were 12 to 19 and 4 to 7 days, respectively (Ritter, 1970; Mcdaniel et al., 2016; Winkel et al., 2017; Herzog et al., 2018). Therefore, we regarded the waterlogging tolerance class of winter and summer crops as class 2 and 1, respectively. The waterlogging tolerance class and time of forests and orchards were determined according to that of poplar and the main fruit trees, respectively (Niinemets and Valladares, 2006; Statistics Bureau of Henan Province and Henan survey team of National Bureau of Statistics, 2019), as shown in Table 2.

2.5.5. Temperature

The average temperature corresponding to the six time periods were calculated according to a nearby meteorological station (34°48′N, 112°28′E) from 2009 to 2019 (National Meteorological Center, 2020), as shown in Table 2.

3. Results and discussion

3.1. Calculation results of flood parameters and geomorphic changes in the inundated area

Only the flood parameters and geomorphic changes of farmland, orchards and forests are shown in Fig. 5. The water depth upstream of *M* is the deepest (Fig. 5a) because the river at *M* is very narrow and there are mountains on both sides. There are plains downstream of *M*, typically causing the velocity upstream of *M* to be larger than that downstream (Fig. 5b), while the flood duration is the opposite (Fig. 5c).

Overall, the areas with large deposition depth are upstream of the inundated area (Fig. 5d), which is consistent with the results of Perignon et al. (2013). Because high flood velocity is more likely to cause erosion, areas with a large erosion depth and high flood velocity are usually near the river (Fig. 5b, d), which has also been found in the previous literature (Xia et al., 2010).

3.2. Calculation results of impacts of extreme floods on plants

3.2.1. Unit risk biomass (URB)

The *URB* corresponding to the six time periods of each mesh was calculated, and the values were averaged (Fig. 6).

The *URB* of the different meshes varies greatly in the inundated area. There are three regions with a high *URB*, namely *R*1, *R*2, and *R*3 (Fig. 6). The reasons causing this phenomenon are shown in Table 3.

3.2.2. Total risk biomass (TRB)

The *TRB* values of the different plants during the six time periods were calculated (Fig. 7).

According to Fig. 7, the change trend of the *TRB* of forests and orchards is similar to that of temperature. This is because for these six influencing factors, the flood parameters during the different time periods are the same, the slight changes in the tree parameters over a year are ignored, and only the significant changes in temperature during the different time periods are considered. The *TRB* values of crops from before and after June 10 change greatly because winter crops are represented before June 10 and summer crops are represented after June 10. The change trend of the *TRB* of crops shifts significantly for different species and time periods, which is different from that of forests and orchards. Therefore, the maximum and minimum *TRB* of crops and those of forests and orchards are during different time periods. Overall, the *TRB* of crops far exceed that of forests and orchards.

The average values of the inundation area, unit biomass, *TRB*, *URB*, and *I* of the different plants during a year were calculated (Table 4). Note that the unit biomass of crops was the average value of summer crops and winter crops, while that of the entire inundated area was the weighted average of all the plants.

According to Table 4, the average inundation area of crops is the largest, which creates the largest impact on the average *TRB*, *URB*, and *I* of the entire inundated area. The average *I* of crops is the biggest, followed by orchards and forests, which is caused by many reasons. Firstly, the average height of crops is the lowest, while that of forests is the highest (Breuer et al., 2003). Secondly, the average waterlogging tolerance of trees is higher than that of crops. The main tree species in the study area is Poplar with an average waterlogging tolerance class of more than 2 (Niinemets and Valladares, 2006), while the primary crop species are wheat and maize, with waterlogging tolerance times of 12 to 19 and 4 to 7 days and waterlogging tolerance classes of 2 and 1, respectively (Mcdaniel et al., 2016; Winkel et al., 2017; Herzog et al., 2018). Moreover, the waterlogging tolerance of other crops are also considerably low (Verhoeven and Setter, 2010). Thirdly, the average maximum rooting depths are 7.0, 5.1, and 2.6 m for trees, shrubs, and herbaceous plants (including most crops), respectively (Gregory, 2010). Therefore, trees are more resistant to erosion than crops.

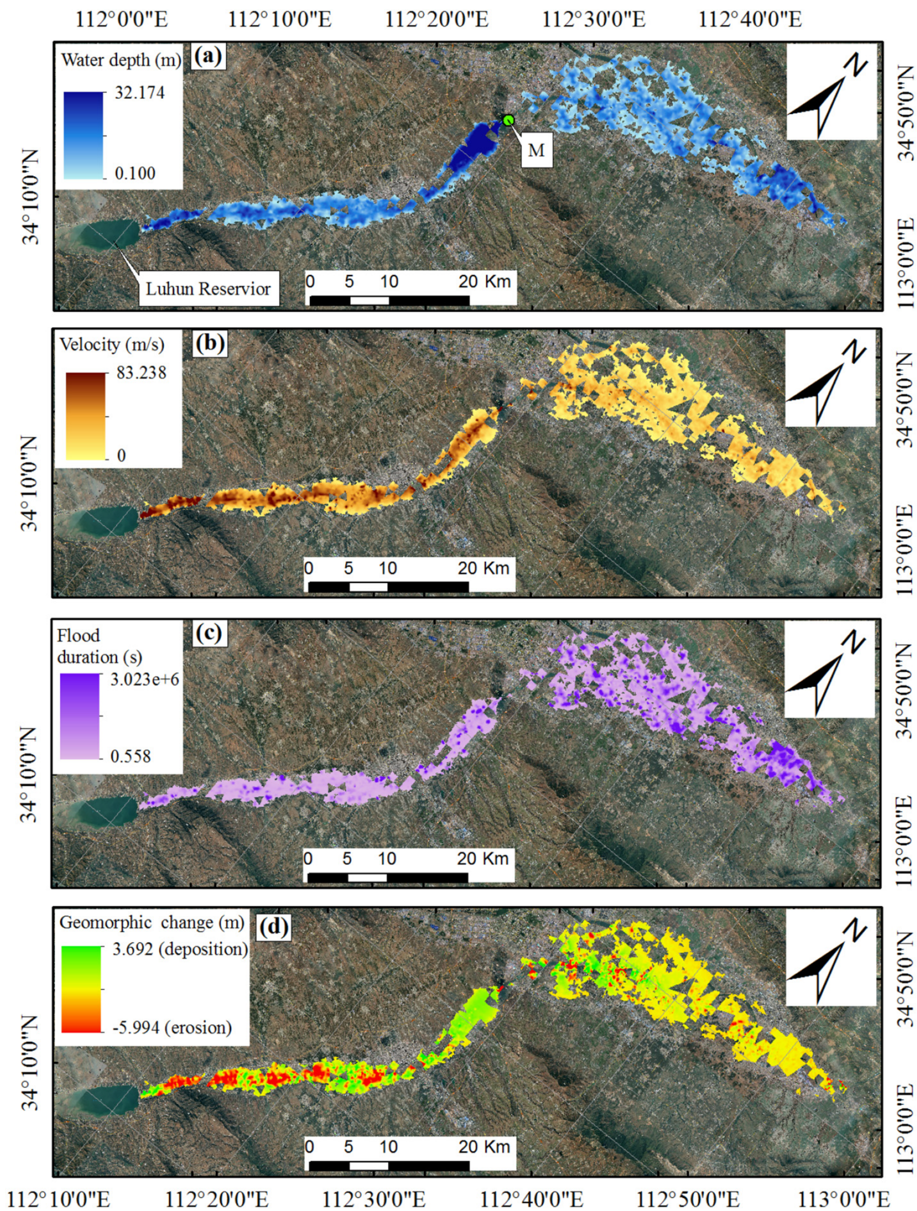

Fig. 5. Flood parameters and geomorphic changes.

3.3. Comparison of results

The results used *URB* and *TRB* to represent the impact degree of extreme floods on plants, which was represented by risk value (0 to 1 or 0 to 100) in previous studies (Kubal et al., 2009; Scheuer et al., 2011; Li et al., 2020). The risk value only considered whether the plant was submerged or not or the vegetation coverage rate, which were not closely related to the plant characteristics. Conversely, both *URB* and *TRB* are based on plant biomass, so they are more appropriate to represent the impact degree.

The results demonstrate the impacts of extreme floods on all plants (crops, arbors and fruit trees) (Figs. 6, 7), while previous literature only focused on several tree species. For example, Stokes (2008) and Karrenberg et al. (2010) respectively analyzed the impact of floods on Salicaceae and black willow species living in the floodplains. Vreugdenhil et al. (2006) analyzed that on *Quercus robur*, *Fraxinus excelsior*, *Crataegus monogyna*, *Salix alba*, *Salix viminalis* and *Populus nigra* in nature reserves. There were also studies that only considered the impact of extreme floods on forests, but ignored crops, shrubs, and grass (Wu et al., 2019). Therefore, the calculation results of this paper could more accurately and comprehensively represent the impacts of extreme floods on all vegetation.

3.4. Study limitations

It was difficult to obtain the actual parameters of a dam-break flood and the characteristics of an extreme flood over the entire inundated area, so we did not verify the models of HEC-RAS and MIKE 21. To ensure the reliability of the model, the parameters used were mean value, test value, or calculated value after the analysis.

We used different maximum impact values to represent the importance of the six influencing factors and proposed methods to calculate their actual impact values according to various situations. Although we comprehensively accounted for the key features of the six influencing factors, there were still subjective judgments. Therefore, to improve the accuracy of the evaluation method, it is necessary to further study the maximum and actual impact values of these influencing factors.

Ignoring other plant species may cause slight errors in the calculation model. However, we used the primary plant species to represent all the plants, e.g., we used poplar to represent forests (accounting for

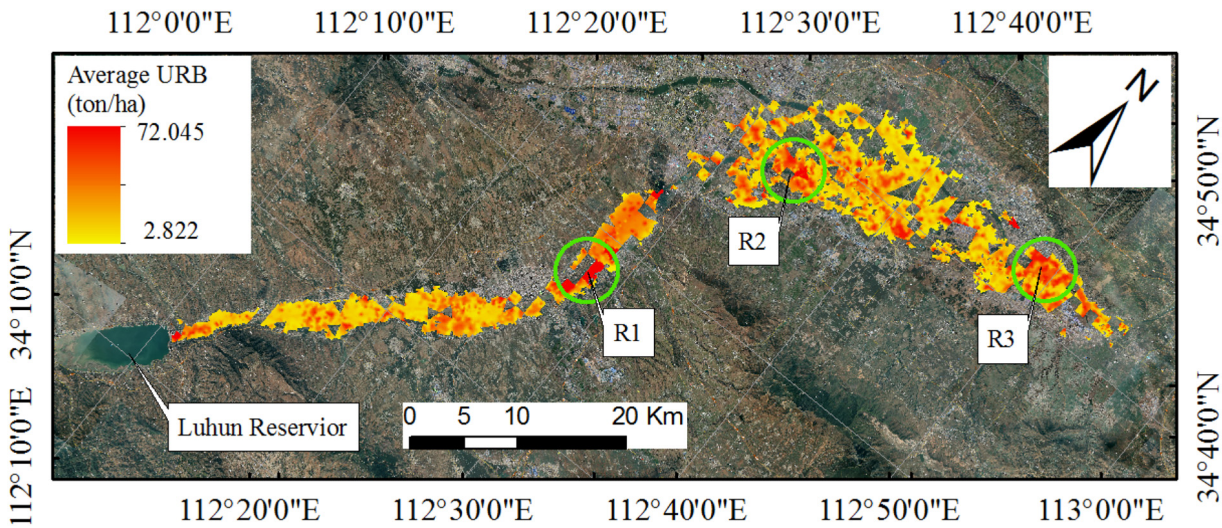

Fig. 6. Average *URB* of each mesh in a year.

Table 3
Reason analysis of high *URB* in *R*1, *R*2, and *R*3.

Position	Deep water depth	High flood velocity	Long flood duration	Large geomorphic change
*R*1	Yes	Yes	No	Yes
*R*2	No	No	Yes	Yes
*R*3	Yes	No	Yes	No

79.46%) (Henan Provincial People's Government, 2018); wheat and rape to represent winter crops (accounting for 75.4%); maize, peanuts, and beans to represent summer crops (accounting for 70.9%); and apple, pear, peach, and grape trees to represent orchards (accounting for 65.5%) (Statistics Bureau of Henan Province and Henan survey team of National Bureau of Statistics, 2019). Therefore, considering the predominant species in the calculation model will cause the error in the results to be negligible.

We used numerous data in the case study to verify the feasibility of the evaluation method, some of which were from our numerical simulation, analysis, and calculation results, while others were from the literature, e.g., the unit biomass of orchards, plant height, ratio of grain to strew, and water content of the grain. Because of the large amount and complexity of data, we did not take measurements in the field or laboratory, which may cause errors in the calculation results.

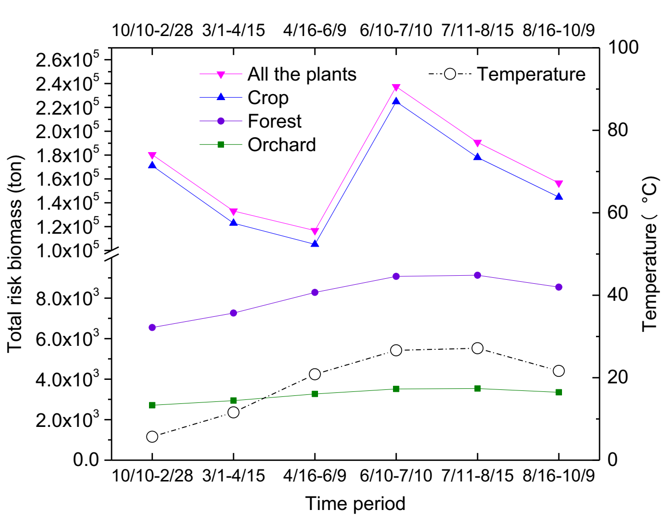

Fig. 7. *TRB* of different plants at different time periods.

4. Conclusions and recommendations

4.1. Conclusions

Extreme floods affect the growth of plants and even cause them to die. Six key factors affect the impacts of flooding on vegetation. We proposed a method to evaluate the impacts of extreme floods on plants, which consisted of two indices of *URB* and *TRB* and the corresponding calculation methods. *URB* and *TRB* can accurately represent the impacts of extreme floods on plants locally and over the entire inundated area, respectively. The calculation of *URB* and *TRB* considered both the six influencing factors and different plant biomass. A case study was used to verify this evaluation method. The results demonstrated that the impacts of extreme floods on plants changed with space and time due to changes in the plant parameters, flood parameters, and temperature.

4.2. Recommendations

We divided a year into six time periods according to the species and growth characteristics of the crops in the study area. If this evaluation method is used in other regions, it is necessary to adjust the time periods according to the local conditions. The maximum *TRB* of all plants occurred during 6/10–7/10, followed by 7/11–8/15. Precipitation in the study area is concentrated in June to August, at which time extreme floods are most likely to happen. Consequently, river managers of Luoyang City should pay more attention to flood control safety during the period of 6/10–8/15. The *URB* and *TRB* of forests and orchards of an area mostly change with the temperature under the same flood conditions (Fig. 7). Therefore, when an extreme flood occurs, the mangers

Table 4
Average inundation area, *TRB*, *URB*, and *I* of different plants.

Plants	Average inundation area (ha)	Unit biomass (ton/ha)	Average *TRB* (ton)	Average *URB* (ton/ha)	Average *I*
Orchards	220.82	35.21	3221.76	14.59	0.41
Forests	334.23	72.05	8141.68	24.36	0.34
Crops	28,799.42	10.58	157,795.95	5.48	0.52
All	29,354.46	11.47	169,132.03	5.76	0.50

of forests and orchards can rapidly assess its impact degree based on the temperature.

Moreover, the most significant cause of the high *TRB* of crops during 6/10–8/15 is the low waterlogging tolerance of maize (Mcdaniel et al., 2016), which is the most widely cultivated summer crop in the study area (Statistics Bureau of Henan Province and Henan survey team of National Bureau of Statistics, 2019). To minimize the adverse impact of extreme floods, we suggest that farmers plant more crops with a high waterlogging tolerance instead of corn, such as rice, sorghum, and sunflower (Malik et al., 2002; Verhoeven and Setter, 2010).

Not only extreme floods, but also many other natural disasters (drought, cyclones, cold waves, heat waves, hurricanes, and debris flows) cause extensive damage to vegetation worldwide (Snyder and Johnson, 2006; He et al., 2019). An accurate assessment of the impacts of these disasters on plants is complex and critical. We propose to use *URB* and *TRB* that are based on plant biomass to represent the impacts of extreme floods on vegetation. These two indices are universal and can be used not only for environmental flood risk assessment but also for an impact assessment of other natural disasters on the plants in any region.

CRediT authorship contribution statement

Yadong Zhang: Conceptualization, Data curation, Formal analysis, Writing – original draft. **Zongkun Li:** Funding acquisition, Project administration, Investigation, Writing – review & editing. **Wei Ge:** Investigation, Writing – review & editing. **Xudong Chen:** Writing – review & editing. **Hongyin Xu:** Writing – review & editing. **Xinyan Guo:** Data curation. **Te Wang:** Visualization.

Declaration of competing interest

The authors declare that they have no known competing financial interests or personal relationships that could have appeared to influence the work reported in this paper.

Acknowledgments

This research was supported by the National Natural Science Foundation of China (Grant No. 52079127, 51679222, 51709239, U2040224), and the Fund of National Dam Safety Research Center (Grant No. CX2021B01).

References

Ahn, C., Moser, K.F., Sparks, R.E., White, D.C., 2007. Developing a dynamic model to predict the recruitment and early survival of black willow (*Salix nigra*) in response to different hydrologic conditions. Ecol. Model. 204 (3–4), 315–325. https://doi.org/10.1016/j.ecolmodel.2007.01.006.

Auchincloss, L.C., Richards, J.H., Young, C.A., Tansey, M.K., 2012. Inundation depth, duration, and temperature influence fremont cottonwood (*Populus fremontii*) seedling growth and survival. West. N. Am. Naturalist. 72 (3), 323–333. https://doi.org/10.2307/41705454.

Beard, J.B., Martin, D.P., 1970. Influence of water temperature on submersion tolerance of four grasses. Agron. J. 62 (2), 257–259.

Ben-Noah, I., Friedman, S.P., 2018. Review and evaluation of root respiration and of natural and agricultural processes of soil aeration. Vadose Zone J. 17, 170119. https://doi.org/10.2136/vzj2017.06.0119.

Bi, Y., 2010. Study on Straw Resources Evaluation and Utilization in China. Chinese Academy of Agricultural Sciences, Beijing.

Breuer, L., Eckhardt, K., Frede, H., 2003. Plant parameter values for models in temperate climates. Ecol. Model. 169, 237–293. https://doi.org/10.1016/S0304-3800(03)00274-6.

Casanova, M.T., Brock, M.A., 2000. How do depth, duration and frequency of flooding influence the establishment of wetland plant communities? Plant Ecol. 147, 237–250. https://doi.org/10.1023/A:1009875226637.

Choi, D.G., Song, J.H., Kang, I.K., 2014. Effect of tree height on light transmission, spray penetration, tree growth, and fruit quality in the slender-spindle system of 'Hongro'/M9 apple trees. Korean J. Hortic. Sci. 32 (4), 454–462. https://doi.org/10.7235/hort.2014.13157.

Copolovici, L., Niinemets, U., 2010. Flooding induced emissions of volatile signalling compounds in three tree species with differing waterlogging tolerance. Plant Cell Environ. 33 (9), 1582–1594. https://doi.org/10.1111/j.1365-3040.2010.02166.x.

DHI Water and Environment, 2007a. MIKE 21 TOOLBOX User Guide.

DHI Water and Environment, 2007b. MIKE 21 FLOW MODEL Hydrodynamic Module User Guide.

DHI Water and Environment, 2007c. MIKE 21 ST User Guide.

Dixon, M.D., 2003. Effects of flow pattern on riparian seedling recruitment on sandbars in the Wisconsin River, Wisconsin, USA. Wetlands. 23 (1), 125–139. https://doi.org/10.1672/0277-5212(2003)023[0125:EOFPOR]2.0.CO;2.

Falloon, P.G., Grogan, R.G., 1991. Effect of root temperature, plant age, frequency and duration of flooding and inoculum placement and concentration on susceptibility of asparagus to phytophthora rot. New Zeal. J. Crop Hort. 19 (3), 305–312. https://doi.org/10.1080/01140671.1991.10421815.

Feng, Y., Song, Z., Zhao, Z., 2009. Collapsible Loess Foundation. Science Press, Beijing, pp. 11–21.

Fraser, L.H., Karnezis, J.P., 2005. A comparative assessment of seedling survival and biomass accumulation for fourteen wetland plant species grown under minor water-depth differences. Wetlands. 25 (3), 520–530. https://doi.org/10.1672/0277-5212(2005)025[0520:ACAOSS]2.0.CO;2.

Gale, M.R., Grigal, D.F., 1987. Vertical root distributions of northern tree species in relation to successional status. Can. J. For. Res. 17 (8), 829–834. https://doi.org/10.1139/x87-131.

Gattringer, J.P., Donath, T.W., Eckstein, R.L., Ludewig, K., Otte, A., Harvolk-Schöning, S., 2017. Flooding tolerance of four floodplain meadow species depends on age. PLoS One 12 (5), e0176869. https://doi.org/10.1371/journal.pone.0176869.

Ge, W., Li, Z., Li, W., Wu, M., Li, J., Pan, Y., 2020a. Risk evaluation of dam-break environmental impacts based on the set pair analysis and cloud model. Nat. Hazards 104, 1641–1653. https://doi.org/10.1007/s11069-020-04237-9.

Ge, W., Sun, H., Zhang, H., Li, Z., Guo, X., Wang, X., Qin, Y., Gao, W., van Gelder, P., 2020b. Economic risk criteria for dams considering the relative level of economy and industrial economic contribution. Sci. Total Environ. 725, 138139. https://doi.org/10.1016/j.scitotenv.2020. 138139.

Ge, W., Wang, X., Li, Z., Zhang, H., Guo, X., Wang, T., Gao, W., Lin, C., van Gelder, P., 2021. Interval analysis of loss of life caused by dam failure. J. Water Resour. Plan. Manag. 147 (1), 04020098. https://doi.org/10.1061/(ASCE)WR.1943-5452.0001311.

Geospatial Data Cloud, Computer network information center of Chinese Academy of Sciences, 2020. GDEMDEM30m. http://www.gscloud.cn/sources/?cdataid=302&pdataid=10. (Accessed 15 May 2020).

Golubkina, N.A., Kharchenko, V.A., Moldovan, A.I., Koshevarov, A.A., Zamana, S., Nadezhkin, S., Soldatenko, A., Sekara, A., Tallarita, A., Caruso, G., 2020. Yield, growth, quality, biochemical characteristics and elemental composition of plant parts of celery leafy, stalk and root types grown in the northern hemisphere. Plants. 9 (4), 484. https://doi.org/10.3390/plants9040484.

Gregory, P.J., 2010. Roots, rhizosphere and soil: the route to a better understanding of soil science? Eur. J. Soil Sci. 57 (1), 2–12. https://doi.org/10.1111/j.1365-2389.2005.00778.x.

Han, Q., Harayama, H., Uemura, A., Ito, E., Utsugi, H., 2017. The effect of the planting depth of cuttings on biomass of short rotation willow. J. Forest Res-JPN. 22 (2), 131–134. https://doi.org/10.1080/13416979.2016.1273084.

He, X., Liang, J., Zeng, G., Yuan, Y., Li, X., 2019. The effects of interaction between climate change and land-use/cover change on biodiversity-related ecosystem services. Global Chall. 3, 1800095. https://doi.org/10.1002/gch2.201800095.

Henan Provincial Department of Forestry, 2015. Present situation of forest resources in Henan Province. http://lyj.henan.gov.cn/2019/07-29/977560.html. (Accessed 21 October 2020).

Henan Provincial People's Government, 2018. Ecological construction planning of forest in Henan Province (2018–2027). http://www.henan.gov.cn/2018/09-21/692208.html. (Accessed 15 August 2020).

Herzog, M., Fukao, T., Winkel, A., Konnerup, D., Lamichhane, S., Alpuerto, J.B., Hasler-Sheetal, H., Pedersen, O., 2018. Physiology, gene expression, and metabolome of two wheat cultivars with contrasting submergence tolerance. Plant Cell Environ. 41, 1632–1644. https://doi.org/10.1111/pce.13211.

Higgisson, W., Briggs, S., Dyer, F., 2018. Responses of nitre goosefoot (Chenopodium nitrariaceum) to simulated rainfall and depth and duration of experimental flooding. Mar. Freshw. Res. 70 (4), 493–503. https://doi.org/10.1071/MF18161.

Hook, D.D., 1984. Waterlogging tolerance of lowland tree species of the south. South. J. Appl. Fo. 8 (3), 136–149. https://doi.org/10.1093/sjaf/8.3.136.

Hu, J., Liu, J., Li, Y., 2008. Practical Technology of Corn Production. Guangdong Science & Technology Press, Guangzhou, pp. 3–4.

Jackson, R.B., Canadell, J., Ehleringer, J.R., Mooney, H.A., Sala, O.E., Schulze, E.D., 1996. A global analysis of root distributions for terrestrial biomes. Oecologia 108 (3), 389–411. https://doi.org/10.2307/4221432.

James, B.B., David, P.M., 1970. Influence of water temperature on submersion tolerance of four grasses. Agron. J. 62, 257–259. https://doi.org/10.2134/agronj1970.00021962006200020024x.

Karrenberg, S., Edwards, P.J., Kollmann, J., 2010. The life history of Salicaceae living in the active zone of floodplains. Freshw. Biol. 47 (4), 733–748. https://doi.org/10.1046/j.1365-2427.2002.00894.x.

Kenow, K.P., Lyon, J.E., 2010. Composition of the seed bank in drawdown areas of navigation pool 8 of the upper Mississippi River. River Res. Appl. 25, 194–207. https://doi.org/10.1002/rra.1118.

Keränen, J., Peuhkurinen, J., Packalen, P., Maltamo, M., 2015. Effect of minimum diameter at breast height and standing dead wood field measurements on the accuracy of ALS-based forest inventory. Can. J. For. Res. 45 (10), 150527143336008. https://doi.org/10.1139/cjfr-2015-0103.

Kramer, K., Vreugdenhil, S.J., Werf, D.C.V.D., 2008. Effects of flooding on the recruitment, damage and mortality of riparian tree species: a field and simulation study on the Rhine floodplain. Forest Ecol. Manag. 255 (11), 3893–3903. https://doi.org/10.1016/j.foreco.2008.03.044.

Kubal, C., Haase, D., Meyer, V., Scheuer, S., 2009. Integrated urban flood risk assessment – adapting a multicriteria approach to a city. Nat. Hazards Earth Sys. 9 (6), 1881–1895. https://doi.org/10.5194/nhess-9-1881-2009.

Li, H., Fa, L., 2011. Height-diameter model for major tree species in China using the classified height method. Scientia Silvae Science 47 (10), 83–90. https://doi.org/10.11707/j.100-7488.20111013.

Li, K., Stella, J.C., Diehl, R.M., Wilcox, A.C., Lightbody, A., Sklar, L.S., 2018a. Can environmental flows moderate riparian invasions? The influence of seedling morphology and density on scour losses in experimental floods. Freshw. Biol. 64 (3), 474–484. https://doi.org/10.1111/fwb.13235.

Li, Z., Li, W., Ge, W., 2018b. Weight analysis of influencing factors of dam break risk consequences. Nat. Hazard. Earth. Sys. 18 (12), 3355–3362. https://doi.org/10.5194/nhess-18-3355-2018.

Li, W., Li, Z., Ge, W., Zhang, H., 2020. Environmental impact evaluation model of dam breach-considering the uncertainty feature of environment. Desalin. Water Treat. 183, 131–138. https://doi.org/10.5004/dwt.2020.25205.

Li, Z., Zhang, Y., Wang, J., Ge, W., Li, W., Song, H., Guo, X., Wang, T., Jiao, Y., 2021. Impact evaluation of geomorphic changes caused by extreme floods on inundation area considering geomorphic variations and land use types. Sci. Total Environ. 754, 142424. https://doi.org/10.1016/j.scitotenv.2020.142424.

Liu, D., Jiang, C., Jia, W., Ge, Y., Gu, L., Zhong, Z., Wu, Y., Li, Z., 1980. Natural Geographical of the World. Higher Education Press, Beijing.

Lugeri, N., Kundzewicz, Z.W., Genovese, E., Hochrainer, S., Radziejewski, M., 2010. River flood risk and adaptation in Europe – assessment of the present status. Mitig. Adapt. Strat. Gl. 15 (7), 621–639. https://doi.org/10.1007/s11027-009-9211-8.

Luo, Y., 2008. Treatment of Collapsible Loess Foundation. China Architecture & Building Press, Beijing, pp. 8–9.

Luoyang Water Resources Surveying and Designing Co., Ltd., 2020. Engineering Geological Survey Report of China Resources Power Shouyangshan Co., Ltd.'s Project of Taking Surface Water from Luohe River Instead of Groundwater. Luoyang Water Resources Surveying and Designing Co., Ltd.

Malik, A.I., Colmer, T.D., Lambers, H., Schortemeyer, S.M., 2002. Short-term waterlogging has long-effects on the growth and physiology of wheat. New Phytol. 153 (2), 225–236. https://doi.org/10.2307/1513791.

Mauchamp, A., Blanch, S., Grillas, P., 2001. Effects of submergence on the growth of phragmites australis seedlings. Aquat. Bot. 69 (2–4), 147–164. https://doi.org/10.1016/S0304-3770(01)00135-8.

Mcdaniel, V., Skaggs, R.W., Negm, L.M., 2016. Injury and recovery of maize roots affected by flooding. Appl. Eng. Agric. 32 (5), 627–638. https://doi.org/10.13031/aea.32.11633.

Meyer, V., Scheuer, S., Haase, D., 2009. A multicriteria approach for flood risk mapping exemplified at the Mulde River, Germany. Nat. Hazards 48 (1), 17–39. https://doi.org/10.1007/s11069-008-9244-4.

Ministry of Housing and Urban-rural Development of the People's Republic of China, General Administration of Quality Supervision, Inspection and Quarantine of the People's Republic of China, 2016. GB50025-2018, Code for Building Construction Collapsible Loess Regions. China Architecture and Building Press, Beijing.

Miyamoto, H., Kimura, R., 2016. Tree population dynamics on a floodplain: a tradeoff between tree mortality and seedling recruitment induced by stochastic floods. Water Resour. Res. 52 (9), 7226–7243. https://doi.org/10.1002/2015WR018528.

Munévar, A., Rubio, G.D., Zurita, G.A., 2018. Changes in spider diversity through the growth cycle of pine plantations in the semi-deciduous Atlantic forest: the role of prey availability and abiotic conditions. Forest Ecol. Manag., S0378112717317814 https://doi.org/10.1016/j.foreco.2018.03.025.

Musgrave, M.E., Ding, N., 1998. Evaluating wheat cultivars for waterlogging tolerance. Crop Sci. 38, 90–97. https://doi.org/10.2135/cropsci1998.0011183X003800010016x.

Najeeb, U., Atwell, B.J., Bange, M.P., Tan, D.K.Y., 2015. Aminoethoxyvinylglycine (AVG) ameliorates waterlogging induced damage in cotton by inhibiting ethylene synthesis and sustaining photosynthetic capacity. Plant Growth Regul. 76, 83–98. https://doi.org/10.1007/s10725-015-0037-y.

National Development and Reform Commission, 2011. Guidelines for Compiling Greenhouse Gases at Provincial Level. pp. 77–79.

National Meteorological Center, 2020. Daily value data set of surface climate data in China (V 3.0). http://data.cma.cn. (Accessed 10 August 2020).

Nicklisch, M., 2004. Abscha¨tzung von Fliebgeschwindigkeiten und ihrer Bedeutung fu¨r Hochwasserscha¨den am Beispiel des August-Hochwassers 2002. (M. S. thesis). Humboldt-Univ., Berlin, p. 109.

Niinemets, U., Valladares, F., 2006. Tolerance to shade, drought and waterlogging in the temperate dendroflora of the Northern hemisphere: tradeoffs, phylogenetic signal and implications for niche differentiation. Ecol. Monogr. 76 (4), 521–547.

Pasley, H.R., Huber, I., Castellano, M.J., Archontoulis, S.V., 2020. Modeling flood-induced stress in soybeans. Front. Plant Sci. 11, 62. https://doi.org/10.3389/fpls.2020.00062.

Perignon, M.C., Tucker, G.E., Griffin, E.R., Friedman, J.M., 2013. Effects of riparian vegetation on topographic change during a large flood event, Rio Puerco, New Mexico, USA. J. Geophys. Res. Earth Surf. 118, 1193–1209. https://doi.org/10.1002/jgrf.20073.

Pires, H.R.A., Cesar Franco, A.C., Piedade, M.T.F., Scudeller, V.V., Kruijt, B., Ferreira, C.S., 2018. Flood tolerance in two tree species that inhabit both the Amazonian floodplain and the dry Cerrado savanna of Brazil. AoB Plants 10 (6), 2041–2851. https://doi.org/10.1093/aobpla/ply065.

Posthumus, H., Morris, J., Hess, T.M., Neville, D., Baylis, A., 2010. Impacts of the summer 2007 floods on agriculture in England. J. Flood Risk Manag. 2 (3), 182–189. https://doi.org/10.1111/j.1753-318X.2009.01031.x.

Pucciariello, C., Voesenek, L.A.C.J., Perata, P., Sasidharan, R., 2014. Plant responses to flooding. Front. Plant Sci. 5, 226. https://doi.org/10.3389/fpls.2014.00226.

Rapacz, M., Ergon, Å., Høglind, M., Jørgensen, M., Jurczyk, B., Østrem, L., Rognli, O.A., Tronsmo, A.M., 2014. Overwintering of herbaceous plants in a changing climate. Still more questions than answers. Plant Sci. 225, 34–44. https://doi.org/10.1016/j.plantsci.2014.05.009 (PMID: 25017157).

Resource and environment data cloud platform, Institute of geographic sciences and natural resources research, CAS, 2020. China's land use remote sensing monitoring data in 2018. http://www.resdc.cn/data.aspx?DATAID=264. (Accessed 27 May 2020).

Ritter, D.B.F., 1970. Flood damage to crops in depression areas of North-central Iowa. Trans. Am. Soc. Agric. Eng. 13 (5), 547–549. https://doi.org/10.13031/2013.38659.

Scheuer, S., Haase, D., Meyer, V., 2011. Exploring multicriteria flood vulnerability by integrating economic, social and ecological dimensions of flood risk and coping capacity: from a starting point view towards an end point view of vulnerability. Nat. Hazards 58 (2), 731–751. https://doi.org/10.1007/s11069-010-9666-7.

Setter, T.L., Waters, I., 2003. Review of prospects for germplasm improvement for waterlogging tolerance in wheat, barley and oats. Plant Soil 253, 1–34. https://doi.org/10.1023/A:1024573305997.

Shi, R., Xie, R., 2009. Practical Cultivation Techniques of Wheat. Zhongyuan farmers Publishing House, Zhengzhou, pp. 11–12.

Shi, L., Zhang, Z.J., Zhang, C.Y., Zhang, J.Z., 2004. Effects of sand burial on survival, growth, gas exchange and biomass allocation of Ulmus pumila seedlings in the Hunshandak Sandland, China. Ann. Bot-London. 94, 553–560. https://doi.org/10.1093/aob/mch174.

Singh, R., Ghildyal, B.P., 1980. Soil submergence effects on nutrient uptake, growth, and yield of five corn cultivars. Agron. J. 72 (5), 737–741. https://doi.org/10.2134/agronj1980.00021962007200050011x.

Snyder, C.D., Johnson, Z.B., 2006. Macroinvertebrate assemblage recovery following a catastrophic flood and debris flows in an Appalachian mountain stream. J. N. Am. Benthol. Soc. 25 (4), 825–840. https://doi.org/10.1899/0887-3593(2006)025[0825:MARFAC]2.0.CO;2.

Statistics Bureau of Henan Province and Henan survey team of National Bureau of Statistics, 2019. Henan Statistical Yearbook-2019. Chinese Statistics Press, Beijing.

Stokes, K.E., 2008. Exotic invasive black willow (*Salix nigra*) in Australia: influence of hydrological regimes on population dynamics. Plant Ecol. 197, 91–105. https://doi.org/10.1007/sl1258-007-9363-0.

Su, Z., Yang, Z., Wang, D., Cai, D., Yao, Y., Lu, J., Zhang, J., 2004. Effect of conservation tillage on water conserving on loess slope-land in west Henan Province. Agric. Res. Arid Areas. 22 (3), 6–8. https://doi.org/10.3321/j.issn:1000-7601.2004.03.002.

Sun, D., Yang, H., Guan, D., Yang, M., Wu, J., Yuan, F., Jin, C., Wang, A., Zhang, Y., 2018. The effects of land use change on soil infiltration capacity in China: a meta-analysis. Sci. Total Environ. 626, 1394–1401. https://doi.org/10.1016/j.scitotenv.2018.01.104.

Tang, Z., Li, B., Cui, J., Li, A., Zhang, L., Wang, T., Chen, P., Hou, L., 2015. Pruning and Management of Fruit Trees. Shandong Science and Technology Press, Jinan, pp. 53–137.

Tebaldi, C., Hayhoe, K., Arblaster, J.M., Meehl, G.A., 2006. Going to the extremes. Clim. Chang. 79, 185–211. https://doi.org/10.1007/s10584-006-9051-4.

The state forestry administration of the People's Republic of China, 2013. Results of the Eighth Continuous Inventory of Forest Resources in Henan Province.

US Army Corps of Engineers, Hydrologic Engineering Center, 2016. HEC-RAS 5.0 2D Modeling User's Manual.

Verhoeven, J.T.A., Setter, T.L., 2010. Agricultural use of wetlands: opportunities and limitations. Ann. Bot-London. 105, 155–163. https://doi.org/10.1093/aob/mcp172.

Vervuren, P.J.A., Blom, C.W.P.M., De Kroon, H., 2003. Extreme flooding events on the Rhine and the survival and distribution of riparian plant species. J. Ecol. 91, 135–146. https://doi.org/10.1002/cjce.5450670329.

Visser, J.M., Peterson, J.K., 2015. The effects of flooding duration and salinity on three common upper estuary plants. Wetlands 35 (3). https://doi.org/10.1007/s13157-015-0644-4.

Vreugdenhil, S.J., Kramer, K., Pelsma, T., 2006. Effects of flooding duration, frequency and depth on the presence of saplings of six woody species in north-west Europe. Forest Ecol. Manag. 236 (1), 47–55. https://doi.org/10.1016/j.foreco.2006.08.329.

Wang, X., Deng, Z., Zhang, W., Meng, Z., Xiao, C., Lv, M., 2017. Effect of waterlogging duration at different growth stages on the growth, yield and quality of cotton. PLoS One 12 (1), e0169029. https://doi.org/10.1371/journal.pone.0169029.

Wang, M., Sun, R., Xiao, Z., 2018. Estimation of forest canopy height and aboveground biomass from spaceborne LiDAR and landsat imageries in Maryland. Remote Sens-Basel. 10 (2), 344. https://doi.org/10.3390/rs10020344.

Watson, E.R., Lapins, P., Barron, R., 1976. Effect of waterlogging on the growth, grain and straw yield of wheat, barley and oats. Aust. J. Exp. Agr. 16 (78), 114–122. https://doi.org/10.1071/EA9760114.

Whitlow, T.H., Harris, R.W., 1979. Flood tolerance in plants: a state-of-the-art review. National Technical Information Service. U.S. Department of Commerce, Washington, D.C., USA.

Winkel, A., Herzog, M., Konnerup, D., Floytrup, A.H., Pedersen, O., 2017. Flood tolerance of wheat – the importance of leaf gas films during complete submergence. Funct. Plant Biol. 44, 888–898. https://doi.org/10.1071/FP16395.

Wu, M., Ge, W., Li, Z., Wu, Z., Zhang, H., Li, J., Pan, Y., 2019. Improved set pair analysis and its application to environmental impact evaluation of dam break. Water 11, 821. https://doi.org/10.3390/w11040821.

Xia, J., Lin, B., Falconer, R.A., Wang, G., 2010. Modelling dam-break flows over mobile beds using a 2D coupled approach. Adv. Water Resour. 33, 171–183. https://doi.org/10.1016/j.advwatres.2009.11.004.

Xu, Y., Zhang, L., Asce, M., 2009. Breaching parameters for earth and rockfill dams. J. Geotech. Geoenviron. 135 (12), 1957–1970. https://doi.org/10.1061/(ASCE)GT.1943-5606.0000162.

Xu, X., Zhang, Q., Tan, Z., Li, Y., Wang, X., 2015. Effects of water-table depth and soil moisture on plant biomass, diversity, and distribution at a seasonally flooded wetland of Poyang Lake, China. Chin. Geogr. Sci. 25 (6), 739–756. https://doi.org/10.1007/s11769-015-0774-x.

Ye, X., Zhang, Q., Bai, L., Hu, Q., 2011. A modeling study of catchment discharge to Poyang Lake under future climate in China. Quat. Int. 244 (2), 221–229. https://doi.org/10.1016/j. quaint.2010.07.004.

Zacks, G., Greet, J., Walsh, C.J., Raulings, E., 2018. The flooding tolerance of two critical habitat-forming wetland shrubs, leptospermum lanigerum and melaleuca squarrosa, at different life history stages. Aust. J. Bot. 66, 500–510. https://doi.org/10.1071/BT18039.

Zaidi, P.H., Rafique, S., Rai, P.K., Singh, N.N., Srinivasan, G., 2004. Tolerance to excess moisture in maize (*Zea mays* L.): susceptible crop stages and identification of tolerant genotypes. Field Crop Res. 90 (2–3), 189–202. https://doi.org/10.1016/j.fcr.2004.03.002.

Zhang, Y., 2018. Study on Characteristics of Forestry Carbon Sequestration and Space-time in Henan Province. North China University of Water Resources and Electric Power, Zhengzhou.

Zheng, Y., Xing, L., 2015. Practical Technology of Modern Agriculture. Hebei Science & Technology Press, Shijiazhuang, pp. 82–92.